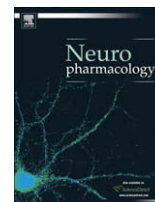




Contents lists available at ScienceDirect

Neuropharmacology

journal homepage: www.elsevier.com/locate/neuropharm

T-type channel blocking properties and antiabsence activity of two imidazo [1,2-*b*]pyridazine derivatives structurally related to indomethacin

Maria Grazia Rimoli^a, Emilio Russo^b, Mauro Cataldi^c, Rita Citraro^b, Paolo Ambrosino^c, Daniela Melisi^a, Annalisa Curcio^a, Salvatore De Lucia^a, Paola Patrignani^d, Giovambattista De Sarro^b, Enrico Abignente^{a,*}

^a Department of Pharmaceutical and Toxicological Chemistry, Faculty of Pharmacy, Federico II University of Naples, Via Domenico Montesano 49, 80131 Naples, Italy

^b Department of Experimental and Clinical Medicine, School of Medicine, University of Catanzaro, Via T. Campanella 115, 88100 Catanzaro, Italy

^c Division of Pharmacology, Department of Neuroscience, School of Medicine, Federico II University of Naples, Via Sergio Pansini 5, 80131 Naples, Italy

^d Department of Medicine and Center of Excellence on Aging, "G d'Annunzio" University, Via dei Vestini, 31, 66013 Chieti, Italy

ARTICLE INFO

Article history:

Received 21 April 2008

Received in revised form

24 October 2008

Accepted 20 November 2008

Keywords:

Imidazopyridazines

Indomethacin

Absence epilepsy

T-type channel

ABSTRACT

It is presently unclear whether the antiseizure effects exerted by NSAIDs are totally dependent on COX inhibition or not. To clarify this point we investigated whether 7-methyl-2-phenylimidazo[1,2-*b*]pyridazine-3-carboxylic acid (DM1) and 6-methoxy-2-phenylimidazo[1,2-*b*]pyridazine-3-carboxylic acid (DM2), two imidazo[1,2-*b*]pyridazines structurally related to indomethacin (IDM) but ineffective in blocking COXs, retain IDM antiabsence activity. When administered by intraperitoneal injection in WAG/Rij rats, a rat strain which spontaneously develops SWDs, both DM1 and DM2 dose-dependently suppressed the occurrence of these seizures. Importantly, these compounds were both more potent in suppressing SWD occurrence than IDM. As T-type channel blockade is considered a mechanism of action common to many antiabsence drugs we explored by whole cell patch clamp electrophysiology in stably transfected HEK-293 the effect of DM1 and DM2 on Cav3.1 channels, the T-type channel subtype preferentially expressed in ventrobasal thalamic nuclei. Both these compounds dose-dependently suppressed the currents elicited by membrane depolarization in these cells. A similar T-type blocking effect was also observed when the cells were exposed to IDM. In conclusion, DM1 and DM2 whilst inactive on COXs, are potent antiabsence drugs. This suggests that compounds with structural features typical of NSAIDs may exert antiepileptic activity independently from COX inhibition and possibly by a direct interaction with T-type voltage-dependent Ca²⁺ channels.

© 2008 Elsevier Ltd. All rights reserved.

1. Introduction

There is an increasing awareness that the pharmacological effects of non-steroidal anti-inflammatory drugs (NSAIDs) are in part independent of the inhibition of cyclooxygenases (COXs) (Tegeger et al., 2001a). For instance, NSAIDs affect the activity of nitric oxide synthase (O'Kane et al., 2003), have free radical scavenger properties (De Gaetano et al., 1985; Mehta et al., 1989) and inhibit the kinase activity IKK β (Yin et al., 1998) thereby repressing NF- κ B activity (Kopp and Ghosh, 1994) and, consequently, the differentiation of immune cells (Matasic et al., 2000) and the expression of adhesion molecules (Pierce et al., 1996; Sakurada et al., 1996) and proinflammatory cytokines (Tegeger et al., 2001b). COX-independent NSAID effects have been observed also on a number of other transductional mediators including MAP kinases, STAT/Jak, p90 rsk and AP-1 (reviewed by Tegeger et al., 2001a). In

addition, the antineoplastic effects of COX-2 inhibitors are largely independent from COX inhibition and may be explained by the ability of these drugs to induce the expression of NSAID-activated gene 1 (NAG-1), a member of the TGF β family which induced apoptosis in cancer cells, and to suppress the expression of the antiapoptotic protein survivin 1 and of carbonic anhydrase (as reviewed by Rigas and Kashfi, 2005). Consistently, COX-2 antineoplastic activity can be observed also in tumor cells not expressing COX; furthermore, NSAID derivatives ineffective on COXs, such as sulindac sulfone, may inhibit cell proliferation (Hanif et al., 1996). Finally, members of the NSAID superfamily do affect the activity of ion channels by a direct interaction with channel subunits, as suggested by the evidence that acid sensitive channels (Voilley et al., 2001) are directly blocked by aspirin, diclofenac, and flurbiprofen, high voltage activated Ca²⁺ channels (Zhang et al., 2007) and voltage gated Na⁺ channel (Park et al., 2007) activity is increased by celecoxib, and chloride channels (Liantonio et al., 2007), KCNQ channels (Peretz et al., 2005) and hERG channels (Malykhina et al., 2002) are activated by fenamates.

* Corresponding author. Tel.: +39 081 678615; fax: +39 081 678612.

E-mail address: abignen@unina.it (E. Abignente).

However, while the role of COX-independent effects in determining the effectiveness of NSAIDs in specific conditions such as pain and cancer is currently under extensive investigation, it remains totally unexplored in other conditions like epilepsy. While, indeed, a number of studies addressed the issue of the role played by arachidonic acid (AA) and prostaglandins (PGs) in various experimental models and found that COX inhibitors decrease seizure frequency and severity in pentylenetetrazole (PTZ)- and kainic acid-induced epilepsy (Dhir and Kulkarni, 2006; Dhir et al., 2006; Tandon et al., 2003), the possible implications of COX-independent mechanisms in determining the efficacy of these drugs has not been explored yet. Structural analogues of classical NSAIDs ineffective on COXs would be powerful instruments to address similar experimental questions by evaluating whether specific pharmacological effects of their parental compounds are retained despite the loss of activity on PG-synthase.

In this perspective, in the present paper we examined the antiepileptic effects of two imidazo[1,2-*b*]pyridazine derivatives, namely 7-methyl-2-phenylimidazo[1,2-*b*]pyridazine-3-carboxylic acid (DM1) and 6-methoxy-2-phenylimidazo[1,2-*b*]pyridazine-3-carboxylic acid (DM2). These molecules belong to a series of heterocyclic compounds, including imidazo[1,2-*a*]pyridines, imidazo[1,2-*a*] and [1,2-*c*]pyrimidines, and imidazo[1,2-*a*]pyrazines (Abignente, 1991), which were synthesized as derivatives of the common general structure shown in Fig. 1a, designed according to the model proposed by Gund and Shen (1977) for the active site of COX.

Such compounds related to structure a) should have the minimal structural features required to act as a COX inhibitor and indeed most of these derivatives showed more or less significant anti-inflammatory and analgesic activity *in vivo* (Abignente, 1991). However, some imidazo[1,2-*b*]pyridazine derivatives (Fig. 1b) including DM1 and DM2 showed peculiar pharmacological properties *in vivo*, namely potent analgesic activity together with low or negligible anti-inflammatory and gastric ulcerogenic actions

(Abignente et al., 1990a,b; Luraschi et al., 1997). These results suggested that the inhibition of PG biosynthesis played at the most a secondary role in the mode of action of imidazo[1,2-*b*]pyridazine derivatives.

Here we show that DM1 and DM2 are completely devoid of COX-1 and COX-2 inhibitory activity, but are effective in suppressing spike and wave discharges (SWDs) in WAG/Rij rats, a genetic rodent model of absence epilepsy, similar to what was recently described for their structural congener indomethacin (IDM), which significantly decreased SWDs in these rats (Kovacs et al., 2006). As T-type channel blockade has been considered as an electrophysiological feature common to antiabsence drugs, we also investigated whether DM1 and DM2 COX-independent antiseizure effect could depend on T-type channel blockade and we found that these compounds are indeed powerful T-type channel blockers and that this property is displayed by IDM as well.

2. Materials and methods

2.1. DM1 and DM2 synthesis

7-Methyl-2-phenylimidazo[1,2-*b*]pyridazine-3-carboxylic acid (DM1) and 6-methoxy-2-phenylimidazo[1,2-*b*]pyridazine-3-carboxylic acid (DM2) were synthesized according to a general procedure, described in Abignente et al. (1990b), consisting in the reaction between an appropriate 3-aminopyridazine and ethyl 2-benzoyl-2-bromoacetate (Br-EBA), which was obtained treating ethyl benzoylacetate with *N*-bromosuccinimide, in the presence of Amberlyst-15 (Meshram et al., 2005). The synthetic method reported here (Fig. 2) was developed modifying the original one described by Abignente et al. (1990a) with the aim of increasing the yield of the final products.

Molecular structures of final and intermediate compounds were confirmed by NMR and MS analyses. ESI mass spectra were recorded with an Applied Biosystems API 2000 whereas ¹H and ¹³C NMR spectra were recorded on a Varian Mercury 400 spectrometer operating at 400 MHz. Chemical shift values are reported in δ units (ppm) relative to tetramethylsilane (TMS) used as internal standard.

Specifically, DM1 was synthesized starting from the commercially available compound 3,6-dichloro-4-methylpyridazine **1a** (1 g, 7 mmol) that was dissolved in

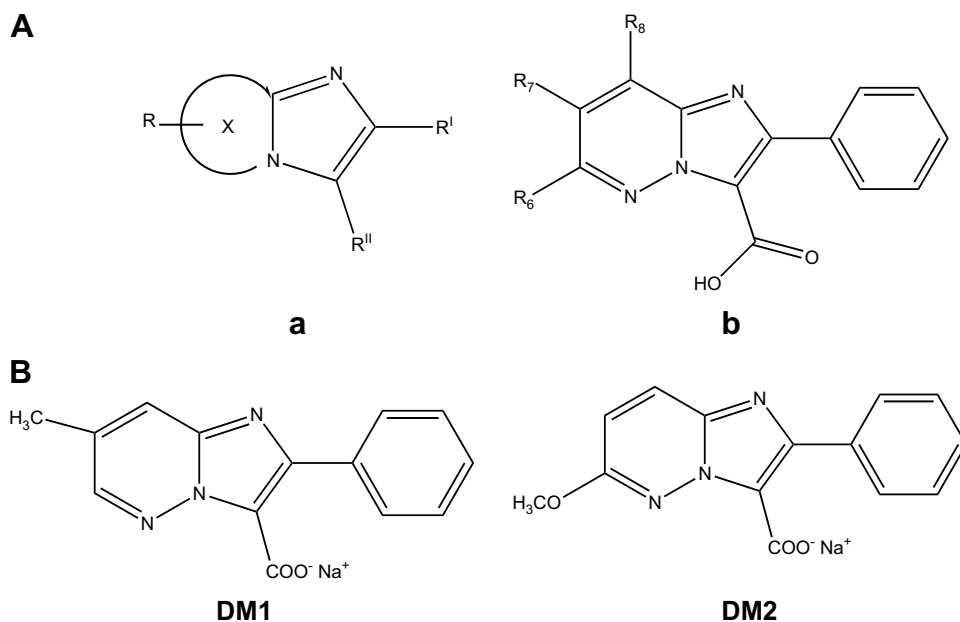


Fig. 1. A. General structural model (a) and chemical structure of imidazo[1,2-*b*]pyridazine derivatives (b). Panel a reports the minimal structure designed by Abignente (1991) to fit into the putative COX active site as described by the Gund and Shen (1977) modelling study. Panel b: general structure of the family of imidazo[1,2-*b*]pyridazine derivatives synthesized by Abignente and coll. based on the minimal structural skeleton reported in panel a. B. Chemical structures of DM1 and DM2. The chemical structures reported were confirmed by NMR and MS analyses. In the case of DM1 the following data were obtained: ¹H NMR in CD₃OD: δ 2.55 (s, 3H, 7-CH₃), 7.48 (m, 3H, Ph), 7.85 (m, 2H, Ph), 8.04 (d, 1H, 8-H), 8.57 (d, 1H, 6-H); ¹³C NMR in CD₃OD: δ 18 (CH₃), 126.7 (8C), 128.7 (4'C), 129.2 (3'C and 5'C), 130.1 (2'C and 6'C), 134.6 (1'C), 135.5 (7C), 136.7 (3C), 143.7 (9C), 149.7 (6C), 159.9 (2C), 171 (CO). MS (EI) *m/z* 276 (M⁺). NMR data for DM2 were the following: ¹H NMR in CD₃OD: δ 4.12 (s, 3H, OCH₃), 7.35 (d, 1H, 7-H), 7.50 (m, 3H, Ph), 7.90 (d, 1H, 8-H), 8.07 (m, 2H, Ph); ¹³C NMR in CD₃OD: δ 54.1 (OCH₃), 122.4 (7C), 125.4 (8C), 128.7 (4'C), 129.2 (3'C and 5'C), 130.1 (2'C and 6'C), 134.6 (1'C), 136.7 (3C), 143.7 (9C), 159.9 (2C), 165.6 (6C), 171 (CO). MS (EI) *m/z* 292 (M⁺).

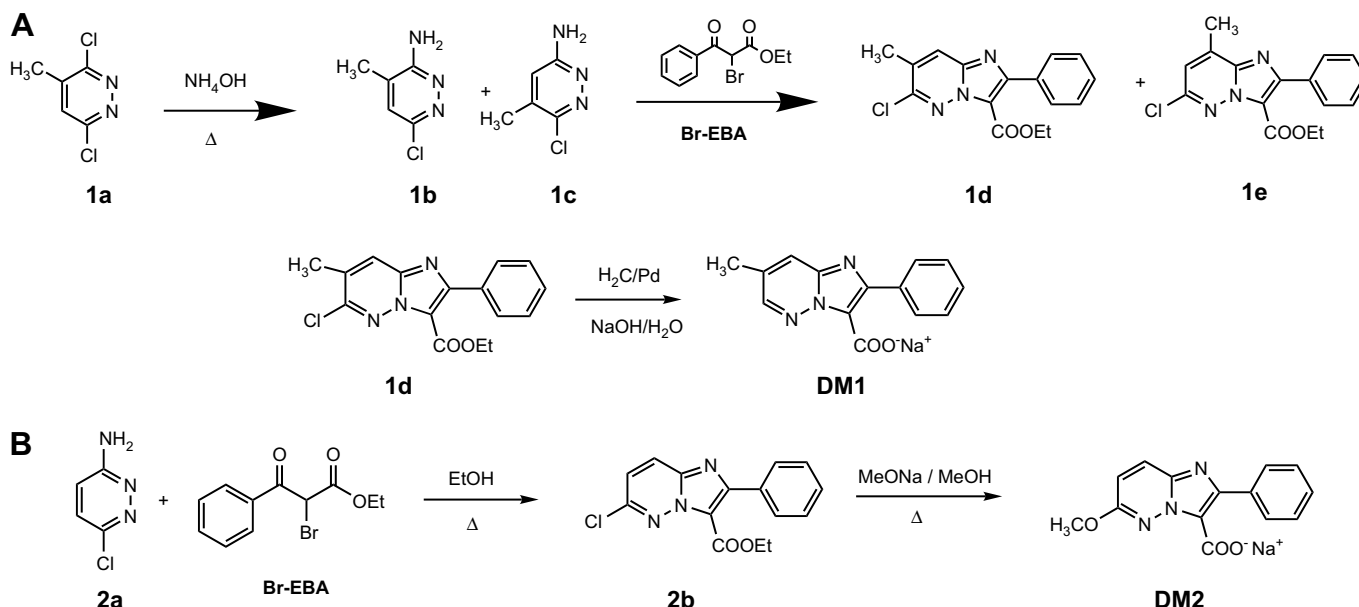


Fig. 2. Chemical synthesis of DM1 (A) and DM2 (B). The panel reports the steps of DM1 and DM2 synthesis detailed in Section 2.

an ethanolic solution of ammonia and was converted into two structural isomers, 3-amino-6-chloro-5-methylpyridazine (**1b**) and 3-amino-6-chloro-4-methylpyridazine (**1c**), through a reaction carried out in autoclave at 150 °C for 10 h. After chromatographic purification, the mixture of these two aminopyridazines (500 mg, 3.48 mmol) was dissolved in anhydrous ethanol, added with an equimolar amount of Br-EBA (943 mg, 3.48 mmol) and refluxed for 5 h. The solvent was then removed *in vacuo*. The residue was dissolved in 10% aqueous HCl and the acid solution was washed with chloroform. The aqueous layer was basified with solid NaHCO₃ and then extracted with chloroform. The organic extract was dried on Na₂SO₄ and evaporated *in vacuo*. Chromatographic separation on silica gel, with dichloromethane as eluent, afforded 300 mg of ethyl 6-chloro-7-methyl-2-phenylimidazo[1,2-*b*]pyridazine-3-carboxylate (**1d**) (0.95 mmol; yield 55%). It was submitted to hydrogenolysis with palladium on ethanolic alkali according to Murakami and Castle (1967). The title compound **DM1** was obtained as sodium salt (100 mg; yield 42%) after hot extractions with anhydrous ethanol.

A similar strategy was used for the synthesis of DM2. In particular, equimolar amounts of 3-amino-6-chloropyridazine (**2a**) (240 mg, 1.85 mmol) and Br-EBA (500 mg, 1.85 mmol) were refluxed for 2 h in anhydrous ethanol. After removing the solvent *in vacuo*, the residue was dissolved in 10% aqueous HCl, washed with chloroform and the aqueous layer was basified with solid NaHCO₃ and extracted with chloroform. The organic extract was dried on Na₂SO₄ and evaporated *in vacuo*. Crystallization from *n*-hexane afforded 250 mg of ethyl 6-chloro-2-phenylimidazo[1,2-*b*]pyridazin-3-carboxylate (**2b**) (0.83 mmol; yield 45%), which was dissolved in methanol and refluxed for 1 h with 2 mL of sodium methoxide. After solvent removal *in vacuo*, hot extractions with anhydrous ethanol yielded DM2 as sodium salt (240 mg; yield 99%).

2.2. *In vitro* cyclooxygenase assay

The effect of DM1, DM2 and IDM (Sigma Chemical Co., St Louis, MO) on COX-1 and COX-2 activities was tested by measuring respectively the concentrations of TXB₂ and PGE₂ released *in vitro* in the presence of these drugs or of their vehicle by peripheral human blood cells collected, after obtaining their informed consent, from three healthy volunteers (2 females and 1 male, aged 29 ± 3 years), who had not taken any NSAID during the two weeks preceding the study. The study protocol was preventively approved by the Ethical Committee of the University of Chieti.

COX-1 activity was measured as described in detail elsewhere (Patrino et al., 1980) by determining the concentration of TXB₂ released by platelets in response to thrombin activation during clotting *in vitro*. In particular, 1 mL blood samples were collected from an antecubital vein, immediately transferred into glass tubes and allowed to clot at 37 °C for 1 h in the presence or in the absence of DM1, DM2 or IDM. Serum was separated by centrifugation (10 min at 3000 rpm) and kept at –80 °C until assayed for TXB₂.

COX-2 activity was measured as previously described by Patrignani et al. (1994) by determining the concentration of PGE₂ released *in vitro* by peripheral blood leukocytes upon exposure to lipopolysaccharide (LPS). Briefly, 1 mL aliquots of peripheral venous blood samples were transferred into heparinized vials (10 i.u. of sodium heparin) and incubated for 24 h at 37 °C in the presence of LPS (10 µg/mL) or saline with or without DM1, DM2 or IDM. The contribution of platelet COX-1 to PG generation was suppressed by pretreating the subjects with 300 mg aspirin po

before sampling. Plasma was then separated by centrifugation (10 min at 2000 rpm) and stored at –80 °C until assayed for PGE₂.

PGE₂ and TXB₂ concentrations were measured by previously described and validated radioimmunoassay (Patrino et al., 1980; Patrignani et al., 1994). Briefly, 4000 d.p.m. of [³H]PGE₂ or [³H]TXB₂ (specific activity >100 Ci/mmol, Perkin Elmer Life Science Products, Brussels, Belgium) were used as radiotracers and incubated in a volume of 1.5 mL with unextracted plasma and serum samples diluted to 1:50–1:30000 in 0.02 M phosphate buffer, pH 7.4 in the presence of specific anti-PGE₂ and anti-TXB₂ at the final concentrations of 1:100000 and 1:120000, respectively. Under our experimental conditions the least detectable concentration was 1–2 pg/mL for both prostanoids.

2.3. Evaluation of IDM, DM1 and DM2 antiepileptic activity

The *in vivo* antiepileptic activity of IDM, DM1 and DM2 was assessed by performing EEG recordings in male WAG/Rij rats (6–7 months old, body weight 250–300 g; Harlan Italy, Correzzana, Milan, Italy), a rat strain that spontaneously develops absence epilepsy. WAG/Rij rats were housed under stable conditions of humidity (60 ± 5%) and temperature (21 ± 2 °C), with free access to food and water and were kept under a reversed light/dark (12/12 h) cycle (light on at 19.00). Animal housing and all the after-mentioned procedures were performed in conformity with the international and national law and policies (European Communities Council Directive, November 24th 1986, 86/609EEC). All efforts were made to minimize animal suffering and to reduce the number of animals used for this protocol.

At least one week before the beginning of the experimentation, a total of five stainless steel screw electrodes were implanted under chloral hydrate anaesthesia (400 mg/kg i.p.; Carlo Erba, Milan, Italy) and with the help of a Kopf stereotaxic instrument on the dura mater: two over the frontal cortex (one for each hemisphere) [AP = 2; L = ±2.5, with skull surface flat and bregma zero-zero (Paxinos and Watson, 1998)], two over the parietal cortex (one for each hemisphere) (AP = –6; L = ±2.5) and a fifth ground electrode over the cerebellum. The electrodes' leads were soldered to a miniature connector which was fixed to the skull with cranio-plastic cement and mounting screws. All animals were left to recover for at least one week and handled twice a day in order to habituate them to experimental manipulation. On the last three days of the recovery time, surface electrodes were connected to an electric swivel mounted on the top of the recording cage housing the animal via a flexible recording cable allowing free animal movements and the animals received daily intraperitoneal injections of saline solution. At the end of the recovery week EEG recordings were performed to identify rats showing bilateral spontaneous SWDs, which were selected to enter the experimentation. SWD displaying rats were randomly assigned to four different groups of 8–10 animals and the animals of each group received, by i.p. injection, three different doses of either IDM (Sigma, Italy), DM1, DM2, or vehicle as detailed in Section 3.

EEG recordings were performed with a multichannel differential amplifier (Astro-Med, West Warwick, USA). EEG signals were amplified and conditioned by analogue filters (filtering: below 1 Hz and above 30 Hz at 6 dB/octave) and subjected to an analogue-to-digital conversion with a sampling rate of 64 Hz. EEG analysis was performed by visual inspection of the recording traces. In particular, SWDs were identified according to the following criteria: a train of generalized spike wave discharges at a frequency of 7–10 Hz, with an amplitude at least double than that of

the background and a duration of at least 1 s. For statistical analysis, the number of SWDs occurring in consecutive 30 min intervals was determined and the means of duration of SWDs occurring in each of these intervals were calculated as described in a previous paper (Russo et al., 2004) and compared by Repeated Measure Anova followed by Bonferroni's posthoc test, $P < 0.05$ was considered significant.

To assess whether any of the drugs in study does induce any change in animal behaviour, each recording session was entirely filmed on videotape and, later on, the tape was independently analyzed by two different experts in animal behaviour, according to the recommendations of van Luijckelaar and Coenen (1986).

2.4. Cell culture and in vitro electrophysiology

T-type Ca^{2+} currents were recorded in HEK-293 cells stably transfected with the $\text{Ca}_v3.1$ isoform of these channels ($\text{Ca}_v3.1$ cells) (courtesy of Dr. E. Perez-Reyes, University of Virginia, Charlottesville, VA, USA), using a fully automated patch clamp workstation (Port-a-patch, Nanion, Munich, Germany) equipped with an HEKA EPC 10 amplifier (HEKA, Lambrecht/Pfalz, Germany). $\text{Ca}_v3.1$ cells were grown in plastic dishes till 75–80% subconfluent in a humidified 5% CO_2 atmosphere using Dulbecco's modified Eagle's medium supplemented with 5% fetal calf serum, 100 IU/mL penicillin, 100 $\mu\text{g}/\text{mL}$ streptomycin, and non-essential aminoacids; they were kept under constant selection with 1 g/L geneticin. Just before starting the recording session, the cells were washed twice with PBS, gently detached from the dish with 5% EDTA in PBS, spinned with a microfuge, washed twice with a solution containing 160 mM NaCl, 4.5 mM KCl, 1 mM MgCl_2 , 2 mM CaCl_2 , 5 mM D-glucose monohydrate, 10 mM Hepes (pH 7.4), and resuspended in 50–100 μL of the same solution. The internal solution contained 75 mM CsCl, 10 mM NaCl, 70 mM CsF, 10 mM EGTA, 2 mM MgCl_2 , 10 mM Hepes, 8 mM glucose (pH 7.4 adjusted with CsOH). The cells were pipetted onto NPC-1 chips and gigaseals were attained with the help of a seal enhancer solution (containing 105 mM NaCl, 4.5 mM KCl, 1 mM MgCl_2 , 40 mM CaCl_2 , 5 mM D-glucose monohydrate, 10 mM Hepes; pH 7.4) by applying the HEK-strong suction protocol. The seal enhancer was extensively washed out and substituted by an external solution containing: 125 mM *N*-methyl- D -glucamine, 10 mM BaCl_2 , 10 mM Hepes and 1 mM MgCl_2 (pH 7.4 adjusted with HCl, osmolarity adjusted to 300 mOsm with sucrose). As IDM, DM1 and DM2 were all dissolved in 0.1% DMSO, this DMSO concentration was routinely added to the external solution in order to prevent any non-specific effect on channel activity due to the solvent. After reaching the whole cell configuration inward Ba^{2+} currents were evoked by delivering consecutive step depolarizations to 0 mV with a 5 s interval between each sweep. To minimize the impact of current run-down, the experimental sessions were started only once the amplitude of these currents became constant over time, which usually occurred by 2 min. As observed in control experiments performed by adding external solution plus vehicle instead of the test drug, once that this condition was attained the currents remained remarkably stable over time.

The drugs under examination, dissolved at the appropriate final concentration in the above described Ba^{2+} containing external solution, were directly pipetted on the chip after removing excess control solution. In order to prevent drug dilution over the chip surface, the drug containing solution was usually pipetted and removed at least twice. Due to the direct drug injection onto the chip, steady state drug effects were typically reached very quickly, in general in 10–20 s.

The PatchMaster software (HEKA, Lambrecht/Pfalz, Germany) was used to generate stimulation protocols and to collect elicited currents. Data were digitised at 20 kHz and filtered online at 10 kHz with the built-in filter of the EPC 10 amplifier. Leak was routinely subtracted by an online P/4 protocol. Offline analysis was performed with the Fitmaster software (HEKA, Lambrecht/Pfalz, Germany), whereas for statistical analysis of data the GraphPad Prism software (GraphPad Software, San Diego, CA, USA) was used.

2.5. Statistical analysis

All data are reported as mean \pm SEM. The Student's test for paired data was used when comparing two data sets, whereas Repeated Measure Anova followed by Bonferroni's posthoc test was used for multiple group comparison. The threshold for statistical significance was set at $P < 0.05$. Statistical comparisons were carried out using the GraphPad 2.04 software suite (GraphPad Software Inc., San Diego, CA, USA).

3. Results

3.1. DM1 and DM2 do not affect the activity of COXs in vitro

To establish whether DM1 and DM2 do possess any significant COX-inhibiting activity, the effect of different concentrations (0.1, 1, 10 and 100 μM) of either the compounds on COX-1 and COX-2 was evaluated respectively by measuring platelet TBX_2 generation in whole blood let to clot at 37 $^\circ\text{C}$ for 1 h and monocyte PGE_2 production in response to LPS *in vitro*, as detailed Section 2. As shown in Fig. 3A and B, DM1 and DM2 did not affect COX-1 and

COX-2 activities up to 100 μM . In contrast, IDM caused a concentration-dependent inhibition of COX-1 and COX-2 activities with IC_{50} values of 0.6 (confidence interval 0.5–0.8) and 0.2 μM (confidence interval 0.1–0.5), respectively. Importantly, the activity of both COX isozymes was almost completely suppressed (>90%) in the presence of 6 μM IDM, a concentration approximately 16-fold lower than the maximal DM1 or DM2 concentration tested (Fig. 3C). These results convincingly show that the two imidazo[1,2-*b*]pyridazines structurally related to indomethacin (IDM) are devoid of COX inhibitory activity.

3.2. DM1, DM2 and IDM decrease number and duration of SWDs in WAG/Rij rats

To establish whether DM1 and DM2, whilst ineffective in blocking COXs, do possess an antiepileptic activity comparable to that of IDM (Kovacs et al., 2006) we compared the effect of these compounds and of IDM on frequency and duration of SWDs in WAG/Rij rats. To this aim SWD displaying rats were randomly assigned to four different groups of 8–10 animals and the animals of each group were i.p. injected with either IDM (Sigma, Italy), DM1, DM2, or vehicle (ethanol/saline 5:95 v/v). Three different doses (1, 5 or 10 mg/kg) of the respective drug were administered to each animal according to a randomized time schedule and surface EEG were recorded for 1 h before injecting each drug dose and continuously for five more hours after each injection. As, in control experiments, we observed that the effect of single drug injections completely disappeared by 48 h from the injection, the different doses were administered to each animal with a three day interval. Fig. 4A reports an example of the SWD that we recorded in WAG/Rij rats.

SWD frequency and duration were quite stable in control animals and were not affected by the injection of vehicle. Conversely, at the doses of 5 and 10 mg/kg i.p. DM1 induced a significant ($P < 0.05$) and dose-dependent decrease in the number and duration of SWDs (Fig. 4B,C). This effect was maximal 120 min after the administration of the higher dose of 10 mg/kg, when SWD frequency averaged approximately 30% (nSWDs = 5.25 ± 1.44 vs 16.39 ± 1.1 ; $p = 0.04$) and duration 40% (dSWDs = 99.67 ± 25.82 vs 230.59 ± 6.23 ; $P < 0.001$) of baseline values, and completely disappeared by 180/210 min after drug injection (Fig. 4B,C). No significant effect ($P = 1.00$) was observed when the lowest dose of 1 mg/kg was administered.

Similarly, DM2 caused a dose-dependent decrease in the occurrence and duration of epileptic SWDs. Differently from what was observed in the case of DM1, the drug was effective at all the tested doses (1, 5 and 10 mg/kg, i.p.) causing a significant ($P < 0.01$) decrease in SWD frequency and duration (Fig. 5). These effects appeared 90 min after administration (2nd epoch), reached a peak at 120 min (nSWDs = 5.75 ± 0.48 vs 17.67 ± 0.68 ; dSWDs = 72.24 ± 6.26 vs 245.49 ± 26.28) and disappeared approximately after 210 min. Interestingly, DM2 was even more potent ($P = 0.048$) than DM1 in reducing SWD duration which averaged approximately 20% of baseline values 120 min after the administration of 10 mg/kg DM2 (vs 40% in case of DM1) (Fig. 5).

Animals treated with either of these compounds did not show significant behavioural changes: rats moved almost continuously around, rearing and pushing the litter during the 300 min after the administration.

To establish whether DM1 and DM2 are as effective as IDM in suppressing SWDs, we performed similar experiments in a group of rats which were injected with three different doses of IDM (1, 5 and 10 mg/kg, i.p.). At the higher tested dose (10 mg/kg) IDM caused a reduction ($P < 0.001$) of both the number and duration of SWDs which averaged 58% (nSWDs = 8.73 ± 1.06 vs 15.09 ± 1.24 control) and 59% (dSWDs = 144.75 ± 8.61 vs 243.16 ± 9.12 control) of

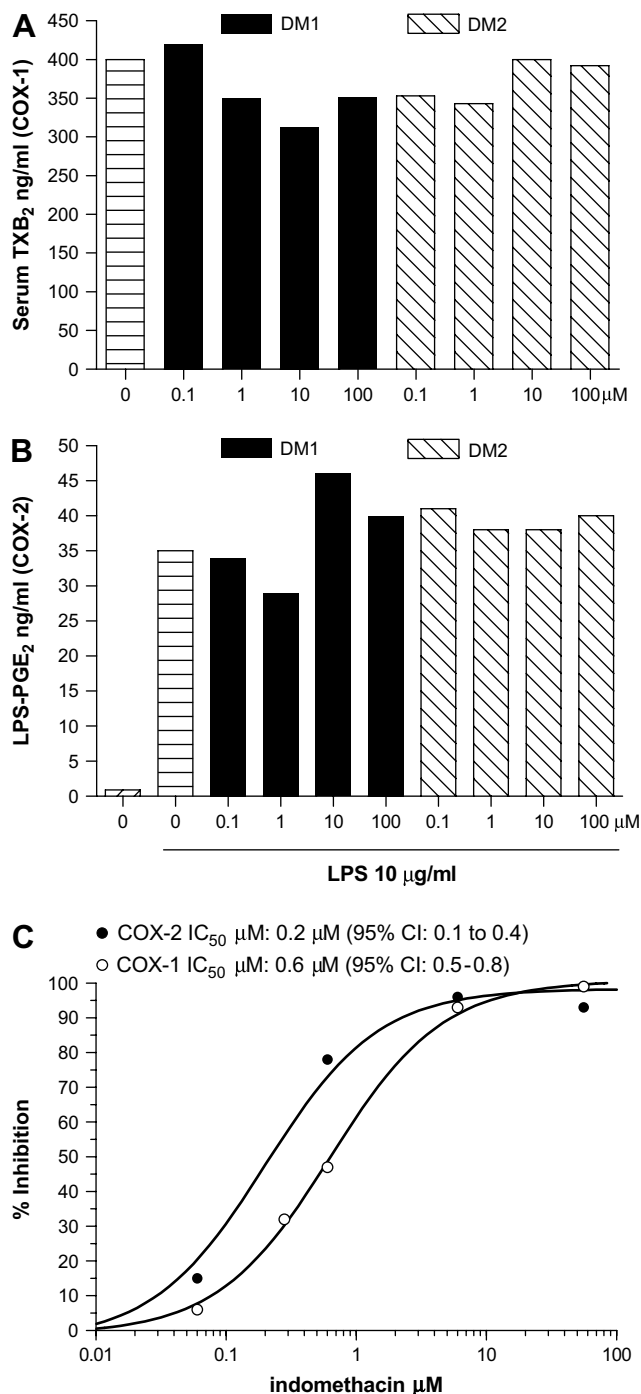


Fig. 3. Effect of DM1, DM2 and IDM on COX-1 and COX-2 activities. The bar graph in panel A reports the TXB₂ concentrations (in ng/ml) measured in serum obtained from whole blood samples collected from healthy human volunteers and let to coagulate *in vitro* in the presence of vehicle (DMSO) or of the reported concentrations of either DM1 or DM2. As discussed in the Section 2 this represents an index of COX-1 activity. Panel B reports the values of the concentrations of PGE₂ released *in vitro* by human monocytes form peripheral blood in the presence of vehicle, vehicle plus 10 μg/ml LPS and vehicle plus DM1 (0.1–100 μM) or DM2 (0.1–100 μM). As discussed in Section 2 this represents a measure of COX-2 activity. Panel C reports the effect of IDM on COX-1 (○) and COX-2 (●) activities determined respectively by measuring TXB₂ generation in recloated peripheral human blood samples and PGE₂ generation by monocytes from peripheral human blood samples exposed to 10 μg/ml LPS, as detailed in the Section 2. The data are expressed as percent inhibition with respect to controls, which were exposed to vehicle (DMSO). Data were fitted to the sigmoidal dose response curve $Y = \min + (\max - \min) / (1 + 10^{(\log(EC_{50} - x)})}$ using the GraphPad software (GraphPad Software Inc., San Diego, CA, USA).

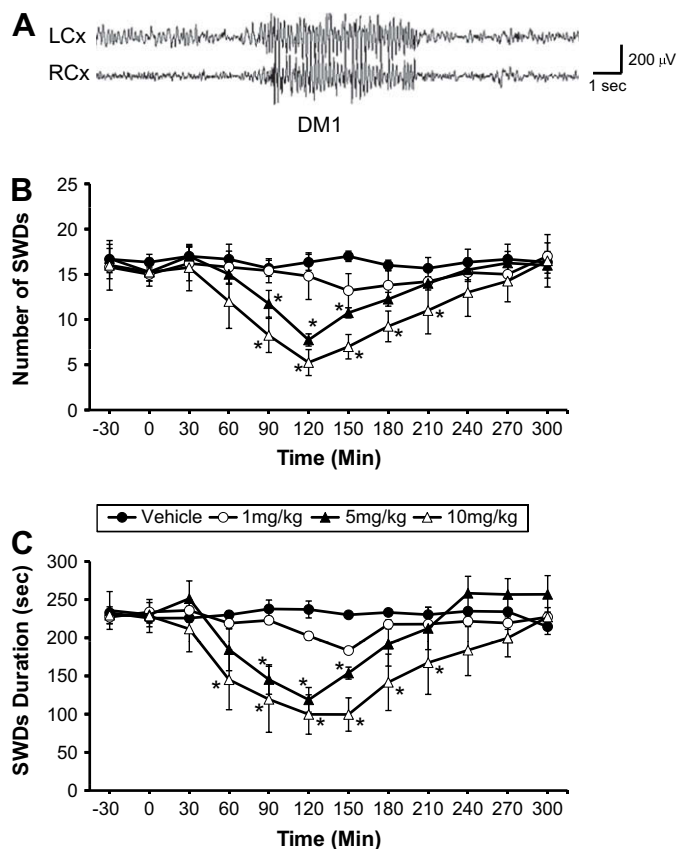


Fig. 4. Effect of DM1 on SWD frequency and duration in WAG/Rij rats. Panel A reports an example of an SWD with a frequency range of 7–9 Hz spontaneously occurring in WAG/Rij rats at the age of 6 months. LCx = left cortex; RCx = right cortex. Panel B reports the time course of the changes in the frequency of SWDs occurring upon the i.p. injection of vehicle (EtOH 5%) or of three different DM1 concentrations (1, 5 and 10 mg/kg) in WAG/Rij rats. SWD frequency is expressed as the number of SWDs occurring during a 30 min interval. Each point in the graph represents the mean ± SEM of the number of SWDs occurring in each animal of the group during the time interval indicated in the x axis of the graph. Panel C reports the time course of the changes in SWD duration (in seconds) occurring upon the i.p. injection of vehicle or of three different DM1 concentrations (1, 5 and 10 mg/kg) in WAG/Rij rats. For each animal we calculated the mean of the duration of all the SWDs occurring during consecutive 30 min intervals. Each point in the graph represents the mean ± SEM of the individual mean duration values of the SWDs during the time interval indicated in the x axis of the graph. As detailed in the text each animal under examination received the injection of vehicle and of all the three drug doses according to a randomized schedule and with an interval of three days between each treatment and the following. * indicates $P < 0.05$ compared to baseline.

baseline respectively (Fig. 6). Thus, IDM was significantly ($P < 0.001$) less effective than both DM1 and DM2 in suppressing SWDs. Furthermore, while, as reported above, a significant anti-absence effect was observed after the administration of 5 mg/kg DM1 and of 1 and 5 mg/kg DM2, IDM was ineffective in suppressing SWDs when administered at both these doses (Fig. 6).

3.3. DM1, DM2 and IDM block Ca_v3.1 channels *in vitro*

To establish whether the anti-absence effects exerted *in vivo* by IDM, DM1 and DM2 depend on T-type channel blockade we investigated by automated whole cell patch clamping the effects of these compounds on the Ba²⁺ currents elicited by step depolarization in HEK-293 stably expressing Ca_v3.1 channels, the T-type channel isoform preferentially expressed in ventrobasal thalamic nuclei.

To explore indomethacin (IDM) effect on Ca_v3.1 channel activity, Ba²⁺ currents were elicited, before and after adding to the chip IDM

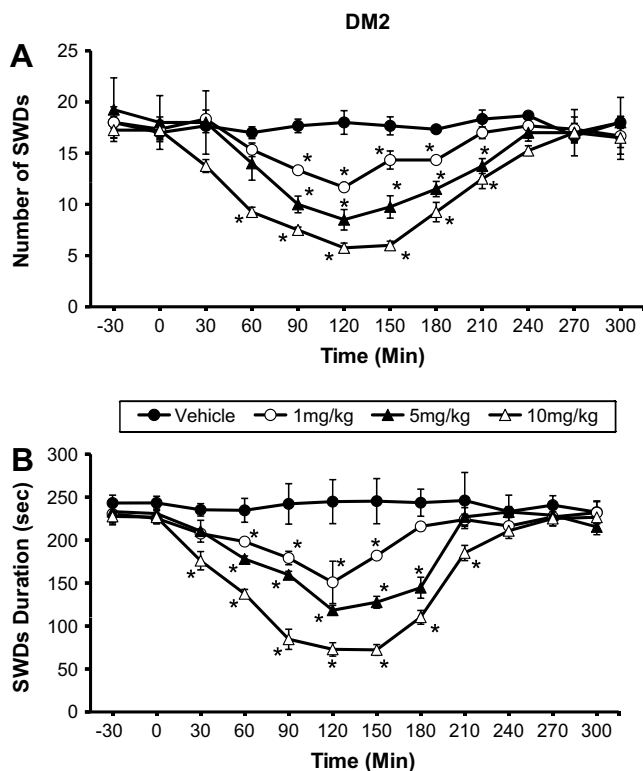


Fig. 5. Effect of DM2 on SWD frequency and duration in WAG/Rij rats. *Panel A* reports the time course of the changes in the frequency of SWDs occurring upon the i.p. injection of vehicle (EtOH 5%) or of three different DM2 concentrations (1, 5 and 10 mg/kg) in WAG/Rij rats. SWD frequency is expressed as the number of SWDs occurring during a 30 min interval. Each point in the graph represents the mean \pm SEM of the number of SWDs occurring in each animal of the group during the time interval indicated in the x axis of the graph. *Panel B* reports the time course of the changes in SWD duration (in seconds) occurring upon the i.p. injection of vehicle or of three different DM2 concentrations (1, 5 and 10 mg/kg) in WAG/Rij rats. For each animal we calculated the mean of the duration of all the SWDs occurring during consecutive 30 min intervals. Each point in the graph represents the mean \pm SEM of the individual mean duration values of the SWDs during the time interval indicated in the x axis of the graph. As detailed in the text each animal under examination received the injection of vehicle and of all the three drug doses according to a randomized schedule and with an interval of three days between each treatment and the following. * indicates $P < 0.05$ compared to baseline.

at progressively higher concentrations (1–30 μ M), by delivering consecutive step depolarizations up to 0 mV from a holding voltage of -80 mV at a 5 s interval. IDM induced a dose-related decrease in the amplitude of the current which averaged $21.5 \pm 5.2\%$ of basal values in the presence of 30 μ M IDM (Fig. 7A,B). Importantly, IDM also modified current kinetics as it significantly accelerated current inactivation (inactivation τ : control: 18.2 ± 1.6 vs 30 μ M IDM: 14.5 ± 1.3 ms; $P < 0.05$) and activation (time to peak: control: 18.2 ± 0.9 vs 30 μ M IDM: 15.0 ± 0.9 ms, $P < 0.01$) (Fig. 7B) suggesting that IDM was affecting channel gating.

When we applied a similar stimulation protocol to $\text{Ca}_v3.1$ expressing cells before and after adding to the recording chip either DM1 (Fig. 8A,B) or DM2 (Fig. 8C,D) we observed that both these drugs induced a rapid block of the inward Ba^{2+} currents elicited by step depolarization. It is worth noticing that both DM1 and DM2 blocked T-type channel at concentrations approximately tenfold higher than IDM. In our specific experimental conditions, which implied the direct injection of the test solution onto the recording chip, we were unable to reverse the effect of all the three drugs tested upon their washout (data not shown).

At the highest concentration used (300 μ M), Ba^{2+} currents averaged $32.3 \pm 2.7\%$ of control values in the presence of DM1 (Fig. 8B) and $39.9 \pm 4.15\%$ in the presence of DM2 (Fig. 8D). As in the

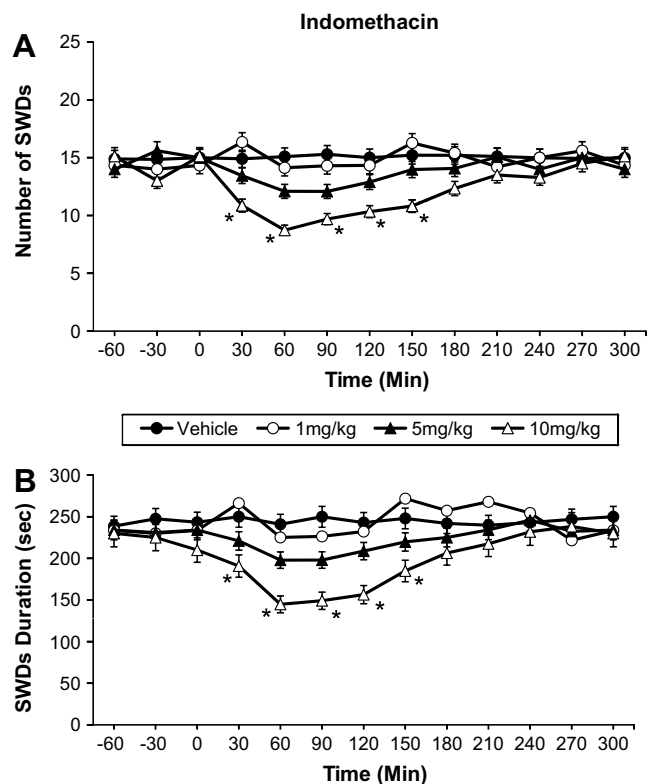


Fig. 6. Effect of IDM on SWD frequency and duration in WAG/Rij rats. *Panel A* reports the time course of the changes in the frequency of SWDs occurring upon the i.p. injection of vehicle (EtOH 5%) or of three different IDM concentrations (1, 5 and 10 mg/kg) in WAG/Rij rats. SWD frequency is expressed as the number of SWDs occurring during a 30 min interval. Each point in the graph represents the mean \pm SEM of the number of SWDs occurring in each animal of the group during the time interval indicated in the x axis of the graph. *Panel B* reports the time course of the changes in SWD duration (in seconds) occurring upon the i.p. injection of vehicle or of three different IDM concentrations (1, 5 and 10 mg/kg) in WAG/Rij rats. For each animal we calculated the mean of the duration of all the SWDs occurring during consecutive 30 min intervals. Each point in the graph represents the mean \pm SEM of the individual mean duration values of the SWDs during the time interval indicated in the x axis of the graph. As detailed in the text each animal under examination received the injection of vehicle and of all the three drug doses according to a randomized schedule and with an interval of three days between each treatment and the following. * indicates $P < 0.05$ compared to baseline.

case of IDM, also DM1 and DM2 hastened current inactivation (inactivation t : DM1: control: 17.4 ± 0.7 vs 300 μ M DM1: 8.4 ± 0.5 , $P < 0.01$; DM2: control: 14.7 ± 1.5 vs 300 μ M DM2: 8.9 ± 1.3 , $P < 0.01$) and current activation (time to peak: DM1: control: 16.5 ± 0.3 vs 300 μ M DM1: 13.5 ± 0.1 , $P < 0.01$; DM2: control: 16.4 ± 0.4 vs 300 μ M DM2: 13.1 ± 0.3 , $P < 0.01$) (Fig. 8B,D).

4. Discussion

The present paper shows that IDM suppresses SWDs *in vivo* in a rat model of absence epilepsy and blocks $\text{Ca}_v3.1$ channels *in vitro*. In addition we report evidence suggesting that both these effects are at least in part independent from COX inhibition as they can be also observed with two indomethacin-like imidazopyridazines DM1 and DM2, which, are ineffective in blocking COXs. This suggests that COX inhibition is neither the only nor the major mechanism responsible for the antiseizure activity of NSAIDs.

A large body of experimental data accumulated in the past show that COX inhibitors possess antiseizure activity in different forms of epilepsy, including absence epilepsy, as shown for IDM by Kovacs et al. (2006) and confirmed in the present study. However, doubts still exist on the intimate mechanism responsible for these effects.

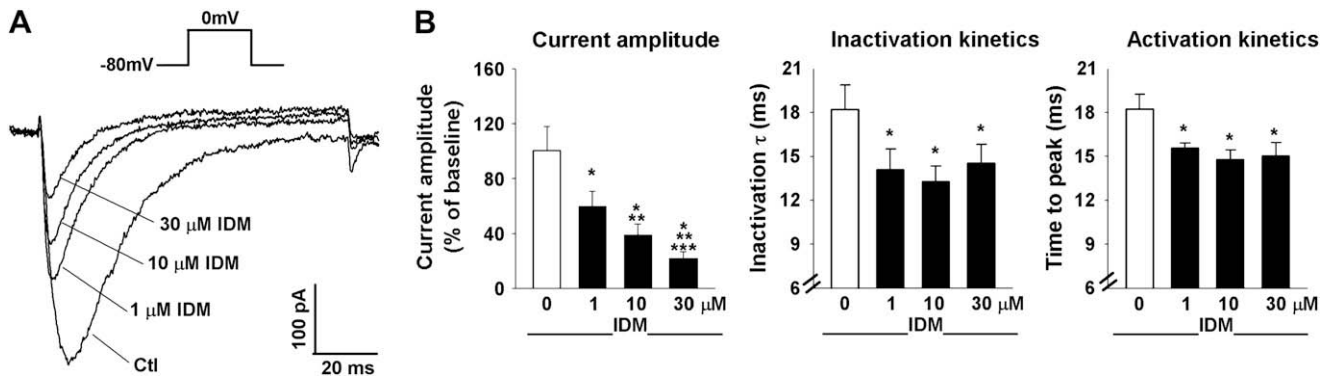


Fig. 7. Effect of IDM on Ba^{2+} currents in Cav3.1 cells. *Panel A* reports the current traces elicited by membrane step depolarization from -80 up to 0 mV, using the protocol reported in figure inset, in a Cav3.1 cell, representative of a group of 6, before and after the exposure to different concentrations of IDM. The bar graph on the left of *panel B* reports the mean values \pm SEM of the amplitude of the currents recorded in the above-mentioned 6 cells at steady state in the presence of each IDM concentration. Data are expressed as percent of the values measured in the absence of the drug. The bar graphs in the middle of *panel B* reports the mean values \pm SEM of inactivation τ (expressed in ms) of the currents recorded at steady state in control condition and in the presence of each drug concentration. Individual inactivation τ s were calculated by fitting in each cell the ascending half of current traces (from peak to zero pA) to the monoexponential equation $I = I_0 \cdot e^{-t/\tau}$ where I is the measured current amplitude, I_0 is current amplitude at peak and t is the time elapsed from peak. The bar graphs on the right of *panel B* report the mean values \pm SEM of the time to peak (in ms) measured from the beginning of step depolarization till the amplitude of maximal inward currents was attained in the presence of the three different IDM concentrations. The traces reported in *panel A* and all the data in *panel B* were obtained once a steady state condition was attained for each drug concentration, which, as described in Section 2 usually occurred in 10–20 s. * $P < 0.05$ vs control, ** $P < 0.05$ vs 1 μ M, *** $P < 0.05$ vs 10 μ M.

As the blockade of voltage gated T-type Ca^{2+} channels has been traditionally considered as a major mechanism of action of anti-absence drugs on the basis of classical electrophysiological evidence (Coulter et al., 1989a,b, 1990) and of more recent work on Cav3.1 knock out mice (Kim et al., 2001; Song et al., 2004), in the present study we investigated whether IDM was effective in blocking these ion channels. In particular, we investigated IDM effect on Cav3.1 channels, which represent the main T-type isoform

responsible for the firing of thalamic relay neurons and whose dysfunction is considered crucial in the genesis of absence epilepsy (as reviewed by Shin et al., 2008). Our finding that IDM potently blocks Cav3.1 channels suggests that that the antiabsence effect of this NSAID (Kovacs et al., 2006) could be at least in part related to T-type channel blockade.

How can this T-type blocking effect be explained? The most obvious mechanism could involve the blockade of PG generation

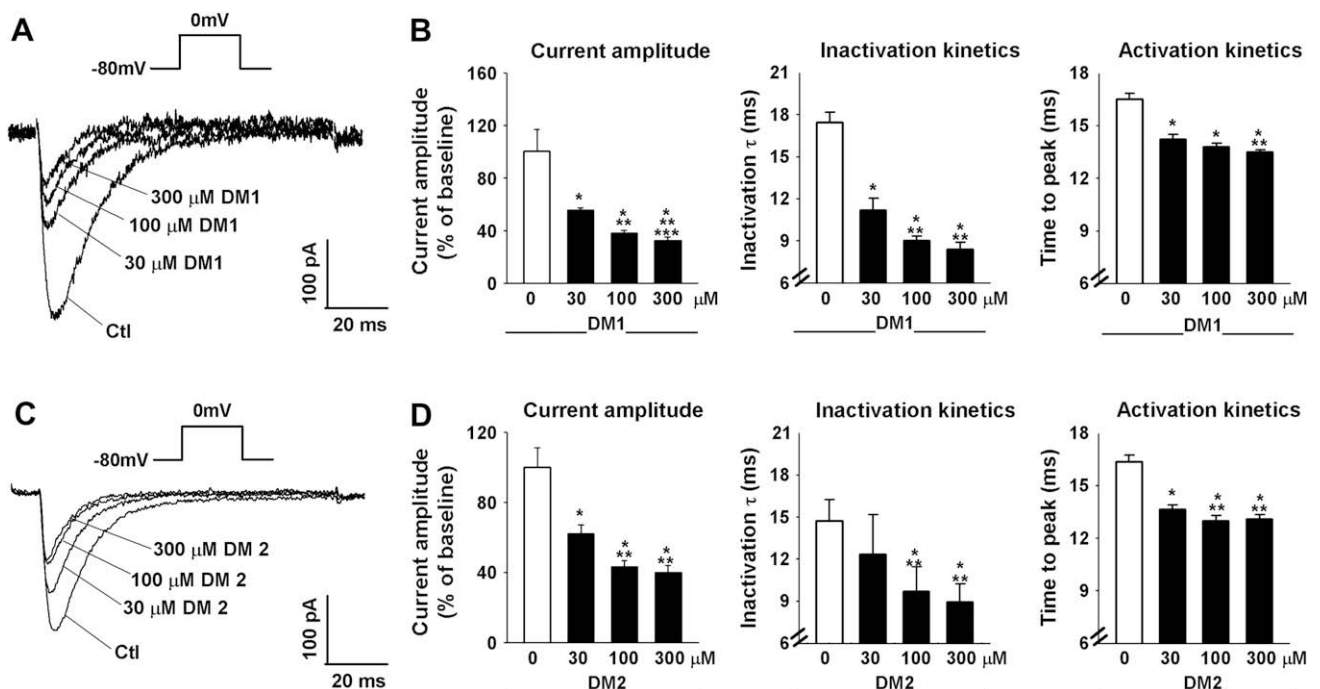


Fig. 8. Effect of DM1 and DM2 on Ba^{2+} currents in Cav3.1 cells. *Panel A* and *C* report current traces elicited by step membrane depolarization from -80 up to 0 mV, according to the protocol reported in figure inset, in two different Cav3.1 cells before and after the exposure to different concentrations of either DM1 or DM2. The two cells are representative of two different groups, each of 6 cells, exposed respectively to DM1 and DM2. The bar graphs in *panel B* and *D* report, as indicated in the figure, on the left, the normalized amplitude of the currents, expressed as percent of the values measured in the absence of the drug, in the middle the inactivation τ (in ms) and on the right the time to peak recorded in the presence of each of the three different concentrations of DM1 or DM2. Each value is the mean \pm SEM of the values obtained in the 6 cells of each group. Inactivation τ s were obtained by monoexponential fitting as described in the legend to Fig. 7. The traces reported in *panels A* and *C* and all the data in *panels B* and *D* were obtained once a steady state condition was attained for each drug concentration, which, as described in the Section 2 usually occurred in 10–20 s. * $P < 0.05$ vs control, ** $P < 0.05$ vs 30 μ M.

due to the IDM-induced COX inhibition. Several evidences support, indeed, the idea that PGs have a role in controlling neuronal excitability and in epileptogenesis. In particular, COX-2 is constitutively expressed in neurons (Yamagata et al., 1993; Breder et al., 1995) especially in dendritic spines (Kaufmann et al., 1996) and, in various models of experimental epilepsy, an increase in COX-2 expression occurs concomitantly with an increase in PG generation (Yamagata et al., 1993; Tocco et al., 1997). In addition, COX-2 expression is markedly and transiently up-regulated in neurons in response to excitatory stimuli such as seizures and kainate (Yamagata et al., 1993; Tocco et al., 1997). Importantly, PGs have been shown to affect the activity of various ion channels and this could have relevant implications in epileptogenesis. For instance, studies on sensory neurons showed that PGE₂ decreases the activity of delayed rectifier K⁺ channels (Evans et al., 1999; Nicol et al., 1997) and shifts the activation curve of the hyperpolarization activated channels I_h in the depolarizing direction thus increasing cell excitability; similar findings have been obtained in hippocampal CA1 pyramidal neurons where PGs have a role in kainate-induced epilepsy (Chen and Bazan, 2005). To the best of our knowledge no previous study has specifically addressed the effect of PGs on T-type channel currents and, thus, the hypothesis that IDM and other NSAIDs could affect the activity of these channels by decreasing PG synthesis remains speculative and could represent an interesting subject of future investigation. A second possible mechanism that could account for IDM-induced decrease in Ca_v3.1 channel activity could be the accumulation of arachidonic acid that NSAIDs induce by blocking the conversion of this fatty acid in PGs. Arachidonic acid has been shown, indeed, to potently inhibit Ca_v3.1 and Ca_v3.2 channel activity *in vitro* (Talavera et al., 2004; Zhang et al., 2000). Interestingly, a significant increase in the expression and activity of PLA₂ and in free fatty acid generation have been observed in epilepsy (Visioli et al., 1993, 1994; Kajiwarra et al., 1996) On the basis of these considerations, we cannot exclude that COX-dependent mechanisms such as a decrease in PG synthesis and an increase in plasmamembrane arachidonic acid concentration could have a role in determining IDM-induced T-type channel blockade. However, the present paper provides strong evidence suggesting that this effect is at least in part independent from COX inhibition. The main argument to support this conclusion is our finding that the ability to block Ca_v3.1 channels is preserved in two imidazopyridazines, DM1 and DM2, structurally related to IDM but unable to block COXs; importantly, these compounds showed a relevant antiabsence activity *in vivo* as well. DM1 and DM2 were synthesized in the 90's in the laboratories of one of the groups participating to the present work as part of a more general project aiming at defining the structural requirements for the pharmacological blockade of COX active site (Abignente et al., 1990a). In particular, they were obtained by modification of a heterocyclic nucleus that was designed to fit with the Gund and Shen (1977) model of COX active site. By performing sequential substitutions on this a large series of molecules provided with the expected COX-dependent anti-inflammatory activity were obtained; however a small group of imidazo[1,2-*b*]pyridazines, including DM1 and DM2, displayed only potent analgesic activity and low or lacking anti-inflammatory activity and ulcerogenic action on rat gastric mucosa which were suggestive of a minimal or null activity on COXs (Abignente et al., 1990a,b; Abignente, 1991; Luraschi et al., 1997). In the present study, we have directly confirmed the lack of the effect of DM1 and DM2 on COX-1 and COX-2 activities. This strongly suggests that other determinants in the NSAID-like skeleton of these molecules diverse from those involved in COX inhibition are responsible for T-type channel blockade and absence seizure suppression. Our finding that COX inhibition is not absolutely required for the antiabsence activity of molecules related to IDM fits well with the growing consensus on the ability of NSAIDs to exert COX-independent pharmacological

effects. Ion channel blockade is probably one of the best examples of such a COX-independent action of NSAIDs. Several published studies already demonstrated that other members of the NSAID superfamily do affect the activity of ion channels by a direct interaction with channel subunits as it has been shown, for instance, for acid sensitive channels (Voilley et al., 2001), high voltage activated Ca²⁺ channels (Zhang et al., 2007), voltage gated Na⁺ channels (Park et al., 2007), chloride channels (Liantonio et al., 2007), KCNQ channels (Peretz et al., 2005) and hERG channels (Malykhina et al., 2002). To the best of our knowledge, our work is the first report suggesting that this could also be the case for T-type channels.

It is important to emphasize that, according to the results of our study, the imidazopyridazines DM1 and DM2 could represent the members of a new class of T-type channel blockers structurally unrelated with those currently available. This could be of interest also in fields unrelated to epilepsy. A considerable interest has been accruing, indeed, on T-type blockers in recent years due to the growing evidence of the involvement of these ion channels in disease processes as different as pain (Shin et al., 2008), cardiac remodelling and arrhythmogenesis (Vassort et al., 2006) and, possibly, cancer growth (Gray and Macdonald, 2006; Panner and Wurster, 2006). Therefore it will be worthy to further investigate the specificity of DM1 and DM2 and their activity in models *in vivo* and *in vitro* of the above-mentioned diseases.

A note of caution is mandatory before concluding that T-type channel blockade is the only or the most relevant factor responsible for the NSAID antiabsence activity. The role of T-type channels in the genesis of this form of epilepsy has been indeed seriously questioned by some authors (Crunelli and Leresche, 2002) and, in this perspective, we cannot exclude that DM1, DM2 or IDM could also affect other ion channels or receptors. The idea that the imidazopyridazines DM1 and DM2 could be acting on other targets besides T-type channels is also suggested by the evidence that they are more potent than IDM in suppressing SWD occurrence *in vivo* despite the higher IDM efficiency in blocking T-type currents *in vitro*. Which could be such an additional imidazopyridazine target? As the structures of DM1 and DM2 have significant similarities with the GABA_A binding drug zolpidem, which is known to suppress SWDs in WAG/Rij rats (Depoortere et al., 1995) an interesting possibility is that these drugs could act on GABA_A receptors. However, preliminary binding studies performed in our laboratories did not show any affinity of either DM1 or DM2 for GABAergic receptors *in vitro* (unpublished data). Therefore further studies will be necessary to identify additional imidazopyridazine targets.

Prospectively, our finding that IDM does exert a potent antiabsence activity and that this activity is preserved in NSAID derivatives ineffective on COXs could be of practical interest. According to the clinical trials reviewed by Posner et al. (2005), approximately 50–70% of patients affected with typical absence epilepsy become seizure-free when treated with the currently available antiabsence drugs, including sodium valproate, ethosuximide and lamotrigine, used in monotherapy. Great uncertainties still exist on how to manage the remaining drug-resistant patients: even though these subjects may benefit out of add-on therapies, some of them, whose numerosity remains indetermined, still have seizures when treated with multiple drugs. To the best of our knowledge, none of the currently available non-steroidal anti-inflammatory drugs has been evaluated yet in controlled clinical trials for its efficacy in drug-resistant absence epilepsy. Nevertheless, serious issues concerning the potential toxicity in paediatric patients, the ability to worsen or induce other types of seizures and to pharmacokinetically interact with antiepileptic drugs, which in various combinations are observed with classical NSAIDs (Burke et al., 2006) limit the further investigation of these compounds. In this perspective, the imidazopyridazines studied in the present work could represent an interesting alternative to classical NSAIDs

and it could be of interest to explore whether, due to the loss of COX-inhibiting activity, they could be safer drugs than classical NSAIDs.

In conclusion, we have shown that two NSAID-related compounds, the imidazopyridazines, DM1 and DM2, possess a significant antiabsence activity despite their ineffectiveness in blocking COX-1 and COX-2, thus suggesting that NSAID antiepileptic activity could be in part independent from COX-blockade. These imidazopyridazines could represent a lead for the development of new antiepileptic drugs to be used in drug-resistant absence epilepsy.

References

- Abignente, E., 1991. Etudes d'imidazo[1,2-a]pyridines et d'analogues doués d'activité anti-inflammatoire. *Actualités de Chimie Thérapeutique* 18, 193–214.
- Abignente, E., Arena, F., Luraschi, E., De Caprariis, P., Marmo, E., Vitagliano, S., Donnoli, D., 1990a. Research on heterocyclic compounds. XXVI. Anti-inflammatory and related activities of some 2-phenylimidazo[1,2-b]pyridazines. *Research Communications in Chemical Pathology and Pharmacology* 67, 43–54.
- Abignente, E., Arena, F., Luraschi, E., Saturnino, C., Marmo, E., Berrino, L., Donnoli, D., 1990b. Research on heterocyclic compounds. XXVII. Synthesis and anti-inflammatory activity of 2-phenylimidazo[1,2-b]pyridazine-3-carboxylic acids. *Farmaco* 45, 1075–1087.
- Breder, C.D., Dewitt, D., Kraig, R.P., 1995. Characterization of inducible cyclooxygenase in rat brain. *Journal of Comparative Neurology* 355, 296–315.
- Burke, A., Smyth, E.M., FitzGerald, G.A., 2006. Analgesic-antipyretic and anti-inflammatory drugs; pharmacotherapy of gout. In: Brunton, L., Lazo, J., Parker, K. (Eds.), *Goodman & Gilman's The Pharmacological Basis of Therapeutics*, 11th ed. McGrawHill Columbus, OH (USA), pp. 671–716.
- Chen, C., Bazan, N.G., 2005. Endogenous PGE₂ regulates membrane excitability and synaptic transmission in hippocampal CA1 pyramidal neurons. *Journal of Neurophysiology* 93, 929–941.
- Crunelli, V., Leresche, N., 2002. Block of thalamic T-type Ca²⁺ channels by ethosuximide is not the whole story. *Epilepsy Currents* 2, 53–56.
- Coulter, D.A., Huguenard, J.R., Prince, D.A., 1989a. Specific petit mal anticonvulsants reduce calcium currents in thalamic neurons. *Neuroscience Letters* 98, 74–78.
- Coulter, D.A., Huguenard, J.R., Prince, D.A., 1989b. Characterization of ethosuximide reduction of low-threshold calcium current in thalamic neurons. *Annals of Neurology* 25, 582–593.
- Coulter, D.A., Huguenard, J.R., Prince, D.A., 1990. Differential effects of petit mal anticonvulsants and convulsants on thalamic neurons: calcium current reduction. *British Journal of Pharmacology* 100, 800–806.
- De Gaetano, G., Cerletti, C., Dejana, E., Latin, R., 1985. Pharmacology of platelet inhibition in humans: implications of the salicylate-aspirin interaction. *Circulation* 72, 1185–1193.
- Depoortere, H., Françon, D., van Lujtelaar, E.L., Drinkenburg, W.H., Coenen, A.M., 1995. Differential effects of midazolam and zolpidem on sleep-wake states and antiepileptic activity in WAG/Rij rats. *Pharmacology, Biochemistry, and Behavior* 51, 571–576.
- Dhir, A., Kulkarni, P.S., 2006. Rofecoxib, a selective cyclooxygenase-2 (COX-2) inhibitor potentiates the anticonvulsant activity of tiagabine against pentylenetetrazol-induced convulsions in mice. *Inflammopharmacology* 14, 222–225.
- Dhir, A., Naidu, P.S., Kulkarni, S.K., 2006. Effect of cyclooxygenase inhibitors on pentylenetetrazol (PZT)-induced convulsions. Possible mechanism of action. *Progress in Neuropsychopharmacology & Biological Psychiatry* 30, 1478–1485.
- Evans, A.R., Vasko, M.R., Nicol, G.D., 1999. The cAMP transduction cascade mediates the PGE₂-induced inhibition of potassium currents in rat sensory neurones. *The Journal of Physiology* 516, 163–178.
- Gray, L.S., Macdonald, T.L., 2006. The pharmacology and regulation of T type calcium channels: new opportunities for unique therapeutics for cancer. *Cell Calcium* 40, 115–120.
- Gund, R., Shen, T.Y., 1977. A model for the prostaglandin synthetase cyclooxygenation site and its inhibition by anti-inflammatory arylacetic acids. *Journal of Medicinal Chemistry* 20, 1146–1152.
- Hanif, R., Pittas, A., Feng, Y., Koutsos, M.I., Qiao, L., Staiano-Coico, L., Shiff, S.I., Rigas, B., 1996. Effects of nonsteroidal anti-inflammatory drugs on proliferation and on induction of apoptosis in colon cancer cells by a prostaglandin-independent pathway. *Biochemical Pharmacology* 52, 237–245.
- Kajiwara, K., Nagawawa, H., Shimizu-Nishikawa, S., Ookuri, T., Kimura, M., Sugaya, E., 1996. Molecular characterization of seizure-related genes isolated by differential screening. *Biochemical and Biophysical Research Communications* 219, 795–799.
- Kaufmann, W.E., Worley, P.F., Pegg, J., Bremer, M., Isakson, P., 1996. COX-2, a synaptically induced enzyme, is expressed by excitatory neurons at post-synaptic sites in rat cerebral cortex. *Proceedings of the National Academy of Sciences of the United States of America* 93, 2317–2321.
- Kim, D., Song, I., Keum, S., Lee, T., Jeong, M.J., Kim, S.S., McEnery, M.W., Shin, H.S., 2001. Lack of the burst firing of thalamocortical relay neurons and resistance to absence seizures in mice lacking alpha1G T-type Ca²⁺ channels. *Neuron* 31, 35–45.
- Kopp, E., Ghosh, S., 1994. Inhibition of NF-κB by sodium salicylate and aspirin. *Science* 265, 956–959.
- Kovacs, Z., Kekesi, K.A., Szilagy, N., Abraham, I., Szekacs, D., Kiraly, N., Papp, E., Csaszar, I., Szego, E., Barabas, K., Peterfy, H., Erdei, A., Bartfai, T., Juhasz, G., 2006. Facilitation of spike-wave discharge activity by lipopolysaccharides in Wistar Albino Glaxo/Rijswijk rats. *Neuroscience* 140, 731–742.
- Liantonio, A., Giannuzzi, V., Picollo, A., Babini, E., Pusch, M., Conte Camerino, D., 2007. Niflumic acid inhibits chloride conductance of rat skeletal muscle by direct inhibiting the CLC-1 channel and by increasing intracellular calcium. *British Journal of Pharmacology* 150, 235–247.
- van Lujtelaar, E.L., Coenen, A.M., 1986. Electrophysiological evaluation of three paradoxical sleep deprivation techniques in rats. *Physiology and Behavior* 36, 603–609.
- Luraschi, E., Arena, F., Sacchi, A., Laneri, S., Abignente, E., Avallone, L., D'Amico, M., Berrino, L., Rossi, F., 1997. Research on heterocyclic compounds. XXXVIII. Synthesis and pharmacological activity of imidazo[1,2-b]pyridazine-2-carboxylic derivatives. *Farmaco* 52, 213–217.
- Malykhina, A.P., Shoeb, F., Akbarali, H.I., 2002. Fenamate-induced enhancement of heterologously expressed HERG currents in *Xenopus* oocytes. *European Journal of Pharmacology* 11, 269–277.
- Matasic, R., Dietz, A.B., Vuk-Pavlovic, S., 2000. Cyclooxygenase-independent inhibition of dendritic cell maturation by aspirin. *Immunology* 101, 53–60.
- Mehta, J.L., Lawson, D.L., Nichols, W.W., 1989. Attenuated coronary relaxation after reperfusion: effects of superoxide dismutase and TXA₂ inhibitor U-63557A. *American Journal of Physiology. Heart Circulation Physiology*, H1240–H1246.
- Meshram, H.M., Reddy, P.N., Sadashiv, K., Yadav, J.S., 2005. Amberlyst-15-promoted efficient 2-halogenation of 1,3-keto-esters and cyclic ketones using *N*-halosuccinimides. *Tetrahedron Letters* 46, 623–626.
- Murakami, H., Castle, R.N., 1967. The synthesis of imidazo[4,5-c]- and v-triazolo[4,5-c]-pyridazines. *Journal of Heterocyclic Chemistry* 4, 555.
- Nicol, G.D., Vasko, M.R., Evans, A.R., 1997. Prostaglandins suppress an outward potassium current in embryonic rat sensory neurons. *Journal of Neurophysiology* 77, 167–176.
- O'Kane, P.D., Queen, L.R., Ji, Y., Reebye, V., Stratton, P., Jackson, G., Ferro, A., 2003. Aspirin modifies nitric oxide synthase activity in platelets: effects of acute versus chronic aspirin treatment. *Cardiovascular Research* 59, 152–159.
- Panner, A., Wurster, R.D., 2006. T-type calcium channels and tumor proliferation. *Cell Calcium* 40, 253–259.
- Park, S.Y., Kim, T.H., Kim, H.I., Shin, Y.K., Lee, C.S., Park, M., Song, J.H., 2007. Celecoxib inhibits Na⁺ currents in rat dorsal root ganglion neurons. *Brain Research* 1148, 53–61.
- Patrignani, P., Panara, M.R., Greco, A., Fusco, O., Natoli, C., Iacobelli, S., Cipolline, F., Ganci, A., Creminon, C., Maclouf, J., Patrono, C., 1994. Biochemical and pharmacological characterization of the cyclooxygenase activity of human blood prostaglandin endoperoxide synthases. *Journal of Pharmacology and Experimental Therapeutics* 271, 1705–1712.
- Patrono, C., Ciabattini, G., Pinca, E., Pugliese, F., Castrucci, F., De Salvo, A., Satta, M.A., Peskar, B.A., 1980. Low dose aspirin and inhibition of thromboxane B₂ production in healthy subjects. *Thrombosis Research* 17, 317–327.
- Paxinos, G., Watson, C., 1998. *The Rat Brain in Stereotaxic Coordinates*, fourth ed. Academic Press, San Diego, CA, USA.
- Peretz, A., Degani, N., Nachman, R., Uziyel, Y., Gibor, G., Shabat, D., Attali, B., 2005. Meclofenamic acid and diclofenac, novel templates of KCNQ2/Q3 potassium channel openers, depress cortical neuron activity and exhibit anticonvulsant properties. *Molecular Pharmacology* 67, 1053–1066.
- Pierce, J.W., Read, M.A., Ding, H., Lusinskas, F.W., Collins, T., 1996. Salicylates inhibit IκB-α phosphorylation, endothelial-leukocyte adhesion molecule expression, and neutrophil transmigration. *Journal of Immunology* 156, 3961–3969.
- Posner, E.B., Mohamed, K., Marson, A.G., 2005. Ethosuximide, sodium valproate or lamotrigine for absence seizures in children and adolescents. *Cochrane Database of Systematic Reviews* 4 Art. No.: CD003032.
- Rigas, B., Kashfi, K., 2005. Cancer prevention: a new era beyond cyclooxygenase-2. *Journal of Pharmacology and Experimental Therapeutics* 314, 1–8.
- Russo, E., Constanti, A., Ferreri, G., Citraro, R., De Sarro, G., 2004. Nifedipine affects the anticonvulsant activity of topiramate in various animal models of epilepsy. *Neuropharmacology* 46, 865–878.
- Sakurada, S., Kato, T., Okamoto, T., 1996. Induction of cytokines and ICAM-1 by proinflammatory cytokines in primary rheumatoid synovial fibroblasts and inhibition by *N*-acetyl-L-cysteine and aspirin. *International Immunology* 8, 1483–1493.
- Shin, H.S., Cheong, E.J., Choi, S., Lee, J., Na, H.S., 2008. T-type Ca²⁺ channels as therapeutic targets in the nervous system. *Current Opinion in Pharmacology* 8, 33–41.
- Song, I., Kim, D., Choi, S., Sun, M., Shin, H.S., 2004. Role of the alpha1G T-type calcium channel in spontaneous absence seizures in mutant mice. *Journal of Neuroscience* 24, 5249–5257.
- Talavera, K., Staes, M., Janssens, A., Droogmans, G., Nilius, B., 2004. Mechanism of arachidonic acid modulation of the T-type Ca²⁺ channel alpha1G. *Journal of General Physiology* 124, 225–238.
- Tandon, M., Anuradha, K., Pandhi, P., 2003. Evaluation of antiepileptic activity of aspirin in combination with newer antiepileptic lamotrigine in mice. *Methods and Findings in Experimental and Clinical Pharmacology* 25, 607–610.
- Tegeder, I., Pfeilschifter, J., Geisslinger, G., 2001a. Cyclooxygenase-independent actions of cyclooxygenase inhibitors. *FASEB Journal* 15, 2057–2072.
- Tegeder, I., Niederberger, E., Israr, E., Gühning, H., Brune, K., Euchenhofer, C., Grösch, S., Geisslinger, G., 2001b. Inhibition of NF-κB and AP-1 activation by R- and S-flurbiprofen. *FASEB Journal* 15, 2–4.

- Tocco, G., Freire-Moar, J., Schreiber, S.S., Sakhi, S.H., Aisen, P.S., Pasinetti, G.M., 1997. Maturation regulation and regional induction of cyclooxygenase-2 in rat brain: implications for Alzheimer's disease. *Experimental Neurology* 144, 339–349.
- Vassort, G., Talavera, K., Alvarez, J.L., 2006. Role of T-type Ca^{2+} channels in the heart. *Cell Calcium* 40, 205–220.
- Visioli, F., Rodriguez de Turco, E.B., Kreisman, N.R., Bazan, N.G., 1994 Jun. Membrane lipid degradation is related to interictal cortical activity in a series of seizures. *Metabolic Brain Disease* 9 (2), 161–170.
- Visioli, F., Rihn, L.L., Rodriguez de Turco, E.B., Kreisman, N.R., Bazan, N.G., 1993. Free fatty acid and diacylglycerol accumulation in the rat brain during recurrent seizures is related to cortical oxygenation. *Journal of Neurochemistry* 61, 1835–1842.
- Voilley, N., de Weille, J., Mamet, J., Lazdunski, M., 2001. Nonsteroid anti-inflammatory drugs inhibit both the activity and the inflammation-induced expression of acid-sensing ion channels in nociceptors. *Journal of Neuroscience* 21, 8026–8033.
- Yamagata, K., Andreasson, K.I., Kaufmann, W.E., Barnes, C.A., Worley, P.F., 1993. Expression of a mitogen-inducible cyclooxygenase in brain neurons: regulation by synaptic activity and glucocorticoids. *Neuron* 11, 371–386.
- Yin, M.J., Yamamoto, Y., Gaynor, R.B., 1998. The anti-inflammatory agents aspirin and salicylate inhibit the activity of $\text{I}\kappa\text{B}$ kinase- β . *Nature* 396, 77–80.
- Zhang, Y., Cribbs, L.L., Satin, J., 2000. Arachidonic acid modulation of α1H , a cloned human T-type calcium channel. *American Journal of Physiology. Heart and Circulatory Physiology* 278, H184–H193.
- Zhang, Y., Tao, J., Huang, H., Ding, G., Cheng, Y., Sun, W., 2007. Effects of celecoxib on voltage-gated calcium channel currents in rat pheochromocytoma (PC12) cells. *Pharmacological Research* 56, 267–274.